ENHANCED KNOWLEDGE IN SCIENCES AND TECHNOLOGY
e-ISSN: 2773-6385

EKST

Vol. 4 No. 2 (2024) 417-427
https://publisher.uthm.edu.my/periodicals/index.php/ekst

# Q-Switched Fiber Laser by Using Spider Web as Saturable Absorber

**Ong Kah Yong[1], Noor Ummi Hazirah Hani Zalkepali[1*]**

[1] *Photonics Devices and Sensor Ressearch Center (PDSR), Department of Physics and Chemistry, Faculty of Applied Sciences and Technology, UTHM Kampus, Cawangan Pagoh, Hab Pendidikan Tinggi Pagoh, KM 1, Jalan Panchor, 86400 Pagoh, Muar, Johor, MALAYSIA*

*Corresponding Author: noorummi@uthm.edu.my
DOI: https://doi.org/10.30880/ekst.2024.04.02.046

**Article Info**

Received: 08 January 2023
Accepted: 14 January 2024
Available online: 12 December 2024

**Keywords**

Spider Silk, Saturable Absorber, Fiber Laser, Q-Switched

**Abstract**

Exploring new saturable absorber (SA) materials with excellent performance to achieve Q-switching operations is a hot topic in laser research. For SA, there are fews techniques to produce Q-switched fiber laser including using a real SA like a semiconductor saturable absorber mirror (SESAM) or an artificial SA like a nonlinear polarisation rotation (NPR), nonlinear optical loop mirror (NOLM), or a nonlinear amplifying loop mirror (NALM). However, there are some drawbacks such as substantial intensity losses, a small operating wavelength, and challenges in optical preparation according to these techniques, therefore, spider web is using as potential SA in this study since the characteristic of spider silk is stronger strength and biocompability. According to the result obtained for spider silk, the modulation depth and saturation intensity was 20.67% and 0.11 MW/cm$^2$ for spider silk. It was also found that the repetition rate raised from 23.3 to 63.3 kHz, while the pulse width has been reduced from 9.173 to 3.889 µs by using laser diode. The signal-to-noise ratio (SNR) for the fundamental frequency is determined to be 63.3 kHz which is calculated to be 56.21 decibels (dB). The highest average output power and pulse energy is 0.074 mW and 1.162 nJ respectively. As a result, the result of the spider silk can be considered as an alternative SA for generation of pulse fiber laser.

## 1. Introduction

Pulsed fiber lasers attract interest when used in certain niche applications such as spectroscopy, fiber-based sensors, biological research, and small-scale manufacturing. Analysts are also seeking higher-quality laser output using a variety of techniques, such as the production of Q-switched fiber lasers, which are extensively used several different commercial uses [1]. When lasers modulate intracavity losses to produce intense short light pulses that are not ultrashort, this process is known as Q switching, which also affects the laser resonator's Q factor.

Q-switching techniques can be used in active or passive ways to create optical pulses in a laser system. Q-switching is an active or passive modulation technology that produces brief pulses with strong peaks. Active Q-switching necessitates electro-optical or acoustic-optical modulators, which ultimately result in substantial cavity loss. Passive Q-switching suffers less than active Q-switching. In comparison to other conventional methods for Q-switching in laser cavities, a passive Q-switched fiber laser utilising a saturable absorber (SA) as a switch is easier, more compact, and more affordable [2]. Since it is simpler to generate the pulsed laser, Q-switching is often a superior method of producing pulses than mode-locking. When there is modulation

intracavity loss, Q-switched lasers produce brief pulses with pulse duration in the microsecond and nanosecond range [3]. An optical modulator is required to regulate the quality factor of the laser cavity (the ratio between the energy stored in the gain medium and the loss each oscillation cycle) to accomplish pulsed operation in fiber lasers [4]. In fiber lasers, Q-switched can be produced with the aid of the saturable absorber (SA). Therefore, there is a tremendous incentive to create new SA types [5]. It is possible to produce a Q-switched fiber laser in a number of ways, including using a real saturable absorber (SA) like a semiconductor saturable absorber mirror (SESAM) or an artificial SA like a nonlinear polarisation rotation (NPR), nonlinear optical loop mirror (NOLM), or a nonlinear amplifying loop mirror (NALM) [1]. Therefore, a passive technique using spider silk as SAs is applied to generate Q-switched fiber lasers.

Semiconductor saturable absorber modulator (SESAM) is the method utilised in the creation of Q-switched that is the most well-known. This method has several disadvantages, including substantial intensity losses, a small operating wavelength, and challenges in optical preparation. Ultrafast recovery times and saturable broadband absorption are two benefits of graphene [6]. The poor absorption co-efficiency and no band gap of only 2% of incident light each layer, two inherent drawbacks of graphene, severely restrict its ability to modulate light and its potential applications in optics-related fields that might call for potent light-matter interactions [7]. Because CNTs are inexpensive and simple to prepare, they are frequently utilised in passively Q-switched lasers. However, the diameters had an impact on the bandwidth and absorption effectiveness [8].

In addition, another group of material as SA for Q-switched lasers in fiber-based systems include transition metal dichalcogenides (TMDCs) and black phosphorous (BP). These group of material have their excellent performance and ultrafast carrier dynamics. However, a majority of these materials encounter certain limitations in addressing the issue of broadband operation. (like TMDCs), easily oxidised under ambient conditions (like BP) [9]. Besides, this material required additional process in synthesis to form an SA. Hence, this work is used spider silk that collected directly from the N. Clavipes to apply as SA without needs another process.

The Pauli exclusion principle states that two or more identical fermions, like electrons, cannot both occupy the same quantum state at the same time. As a result, there are a limited number of places for electrons in a semiconductor's conduction band. When a SA material is exposed to bright light and the ground-state absorption is greater than the excited-state absorption, electrons from the valence band are activated and fill the conductance band. The utilization of spider silk as saturable absorbers stems from its unique combination of robust strength and biocompatibility. Spider silk, renowned for its exceptional tensile strength, provides a durable and resilient material for applications in saturable absorbers. This inherent strength allows spider silk to effectively withstand and modulate the intensity of light pulses, making it an ideal candidate for optical devices and laser systems. Additionally, the biocompatible nature of spider silk enhances its versatility, enabling its integration into various biological and medical applications without adverse effects. Thus, the distinctive properties of spider silk not only contribute to its efficacy in optical technologies but also broaden its potential applications in fields where biocompatibility is crucial.

## 2. Methods and Characterization of spider silk

The two female N.Clavipes spiders taken for silk collecting. Two non-gravid adult and sub-adult spiders is mixed together. The spider silk was fabricated by using mechanical attachment techniques before employing in single ring cavit design.

Fig. 1 depicts the arrangement used to assess the performance of a laser diode pump operating at a wavelength of 980nm. A laser diode is connected to an optical power metre, with a 980nm wavelength serving as the pumping source. However, in this experimental setup, only wavelengths of 980 nm are used to characterise pump

Prior to coupling the laser diode from Thorlabs with the Wavelength Double Multiplexer (WDM), there are two distinct wavelengths available: 980nm and 1550nm, as shown in Fig. 2. The Wavelength Division Multiplexer (WDM) is then connected to a 3-meter-long Erbium Doped Fibre (EDF), which is in turn connected to an Isolator. The current flows in accordance with the direction of the isolator. The outcome of the spectrum graph was displayed on the Optical Spectrum Analyzer (OSA).

In Fig. 3, the laser diode is linked to a Wavelength Double Multiplexer (WDM) and connected to a 3-meter-long Erbium Doped Fibre. The isolator is subsequently linked to a coupler, with 90% of the signal being coupled to the output of the Wavelength Double Multiplexer, while the remaining 10% is coupled to the Optical Spectrum Analyzer to display the output spectrum.

The fibre laser system, seen in Fig. 4, consists of two wavelengths: 980nm and 1550nm. However, the laser diode utilises the 980nm wavelength as the pumping source. A laser diode is connected to a fused wavelength division multiplexer (WDM) with a wavelength of 980 nm. The wavelength division multiplexer is linked with an erbium-doped fibre (3.0m) and thereafter connected to the isolator (ISO). The isolator is connected to the spider silk-SA and subsequently to the coupler. The coupler splits the signal, with 90% of the output port going to the

Enhanced Knowledge in Sciences and Technology Vol. 4 No. 2 (2024) p. 417-427

WDM and the remaining 10% going back to the coupler. The coupler splits the output port into two equal parts, with 50% going to the OSA and the other 50% going to the OSC.

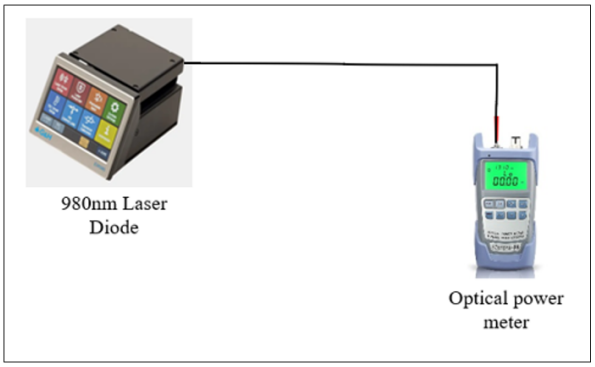


**Fig. 1** *Experimental design to characterised nonlinear laser diode at wavelength of 980nm*

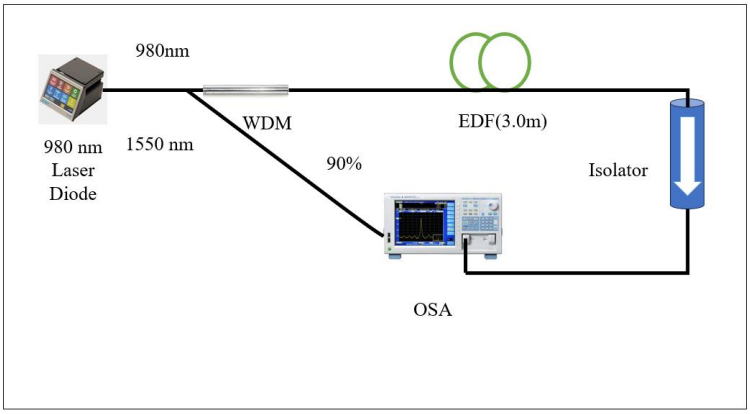


**Fig. 2** *Experimental design to characterised erbium-doped fiber*

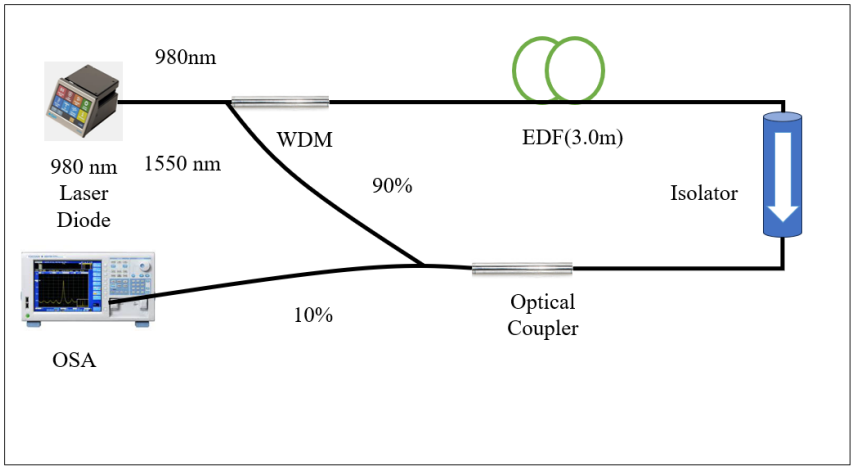


**Fig. 3** *Experimental design to characterised single ring fiber laser*

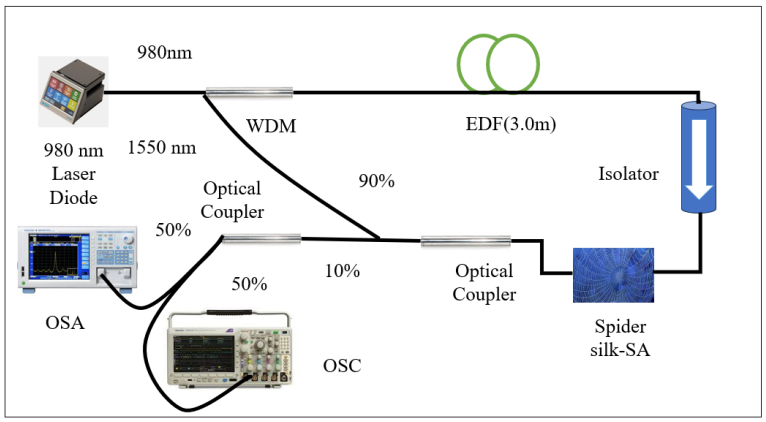


**Fig. 4** *Experimental design of Q-switched fiber laser using spider silk at wavelength of 980nm*

## 3. Results and Discussions

### 3.1 Ultraviolet-visible, SEM, FTIR, Nonlinear absorption

Fig. 5 presents the absorbance spectrum observed within the wavelength range of 200 nm to 800 nm. The absorption peak of spider silk is observed to be approximately 5.609 at a wavelength of 285 nm. This observation underscores the potential utility of spider silk in the field of ultrafast photonics, specifically within the telecommunication range of approximately 300 nm.

Fig. 6 displays SEM images of spider silk, captured at a magnification of 2,000 times. The analysis indicates that the nanofibrils acquired exhibit a notably organised arrangement, playing a pivotal role in dictating the mechanical properties of various biological substances, such as spider silk. The morphology of spider silk, comprising twisted nanofibril bundles, was revealed through the utilisation of SEM. The nanofibrils exhibited interconnectivity, and when subjected to stretching, the formation of nano-cracks occurred instead of significant cracks. The exceptional toughness and strength of nanofibrils can be attributed to their evident connectivity.

Furthermore, Fig. 7 illustrates the EDX spectrum, accompanied by a table presenting the tabulated data of the elements. The utilisation of EDX analysis confirmed the purity of the spider silk SA, as evidenced by the elemental composition obtained from the EDX spectrum. The elemental composition acquired comprises carbon, oxygen, nitrogen, and sulphur. The carbon element exhibits the highest atomic percentage in comparison to other elements

Fig. 8 shows a FTIR analysis was conducted to investigate the chemical constituents present in the synthesised spider silk. Fig. 8 displays the FTIR absorbance spectrum of spider silk, acquired within the wavenumber range of 400-4000 $cm^{-1}$. The absorbance spectrum exhibits multiple peaks at various positions. The observed peaks at 1266, 1101, 1019, 873, and 639 $cm^{-1}$ are indicative of the C-O stretching vibrations. The peaks observed at 1717, 2860, 2930 are indicative of the functional groups C=O, H-C-H respectively.

Fig. 9 illustrates the nonlinear absorption characteristics of spider silk. The figure represents the relationship between the modulation depth and saturation intensity, which are measured at 20.67% and 0.11 $MW/cm^2$, respectively. The findings of this study validate that spider silk is comparable to other SA materials in terms of its suitability for pulse fibre laser applications, despite having a slightly lower energy bandgap value compared to other SA [10].

Enhanced Knowledge in Sciences and Technology Vol. 4 No. 2 (2024) p. 417-427

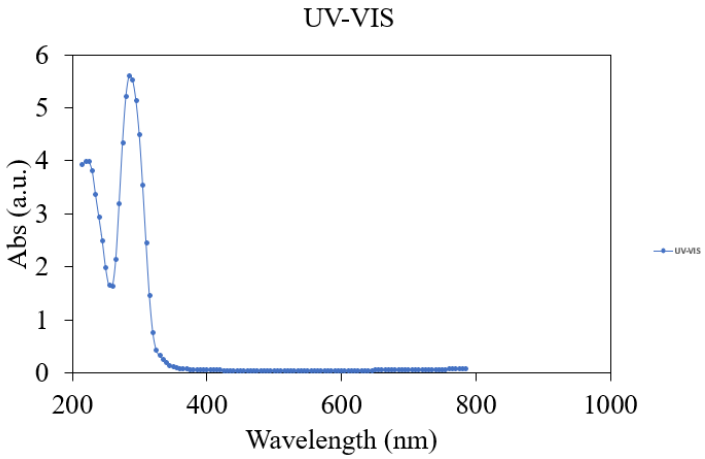


**Fig. 5** *Absorbance spectrum observed from 200 nm to 1000 nm*

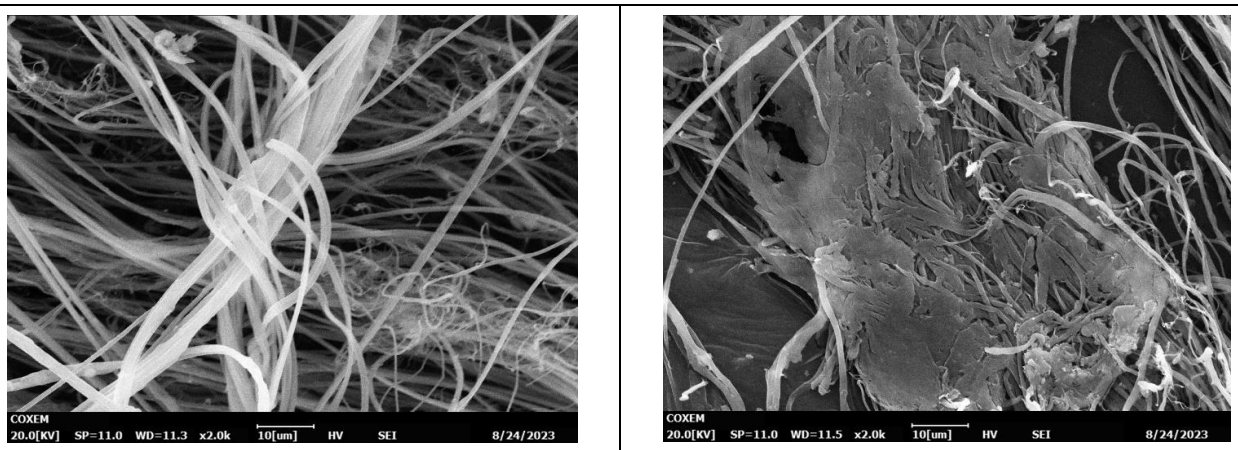


**(a)** **(b)**

**Fig. 6** *SEM images: (a) Raw spider silk with the corresponding EDX elemental analysis shown (b)Spider silk with a high magnification image corresponding EDX elemental analysis*

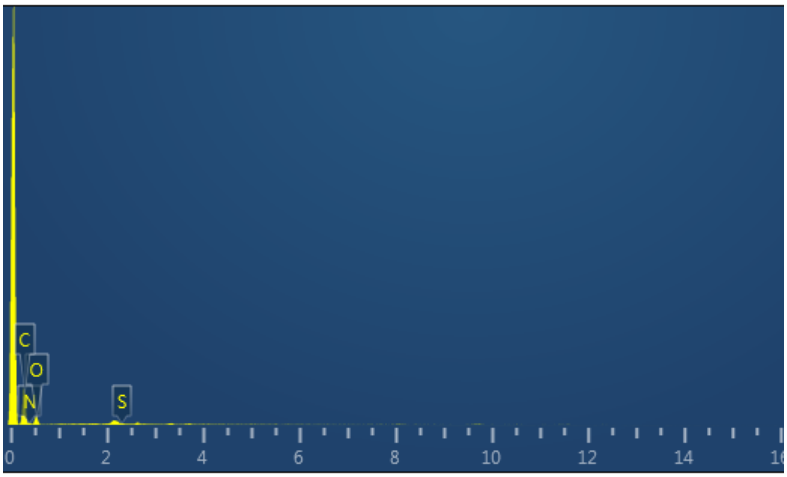


**Fig. 7** *Spectrum of element carbon, oxygen, nitrogen and sulfur*

**Table 1** *Spectrum of element composition obtained such as carbon, oxygen, nitrogen and sulfur*

| **Spectrum 1** | | | | |
|---|---|---|---|---|
| **Element** | **Line Type** | **Weight %** | **Weight % Sigma** | **Atomic %** |
| O | K series | 29.33 | 1.61 | 24.76 |
| C | K series | 44.34 | 1.80 | 49.85 |
| N | K series | 26.33 | 2.53 | 25.39 |
| S | K series | 0.00 | 0.09 | 0.00 |
| Total | | 100.00 | | 100.00 |

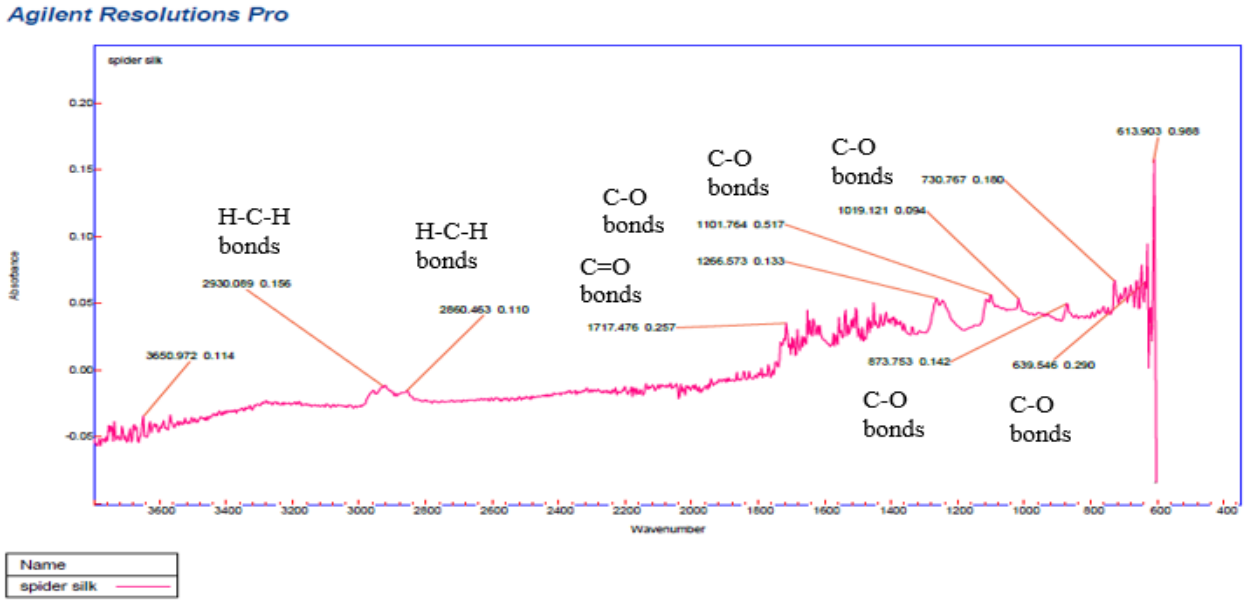


**Fig. 8** *Fourier Transform Infrared Spectroscopy of spider silk*

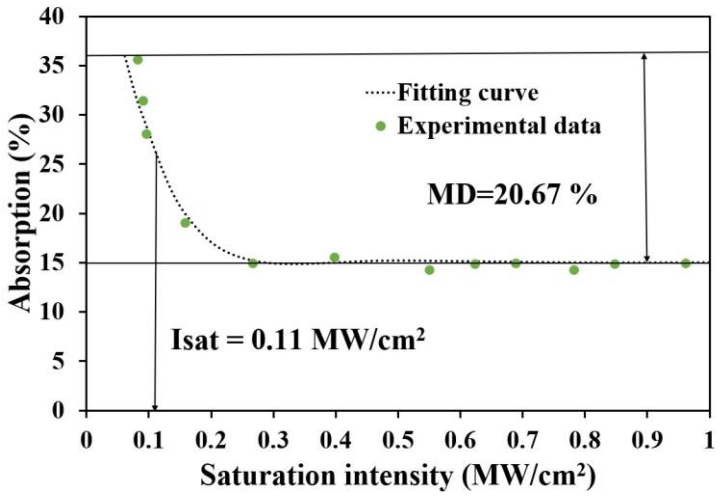


**Fig. 9** *Nonlinear optical absorption of spider silk*

Enhanced Knowledge in Sciences and Technology Vol. 4 No. 2 (2024) p. 417-427

## 3.2 Characterization of laser diode, erbium doped fiber, single ring fiber laser

Fig. 10 depicts the graphical representation of the correlation between the current and input pump power for a laser diode operating at a wavelength of 980nm.The magnitude of the current is directly proportional to the magnitude of the input pump power. Hence, it can be observed that the relationship between the two variables exhibits a linear trend, wherein the current demonstrates a proportional increase with the corresponding increase in input pump power. The current attained its maximum value of 500mA.

Fig. 11 shows the spectral response of amplified spontaneous emission (ASE) for EDF by varying the pump power from 38.70mW to 219.40mW. The output power is -34.027 dBm and a central wavelength of approximately 1558.4 nm. In this experimental study, the erbium-doped fibre (EDF) laser initiates the continuous wave (CW) mode when the pump power reaches a value of 38.70mW. A transition from continuous wave (CW) to pulse regime is observed when the pump power reaches 129.10 mW, resulting in a power level of -44.231 dBm. The system's observability persists until the pump power reaches 219.40 mW, with the operating wavelength approximately at 1559.2 nm and peak power at -34.017 dBm, as depicted in Fig. 12 [11].

The Q-switching phenomenon in a fibre laser was observed when the pump power reached a value of 14.10 mW. The Q-switched spectrum was examined using an optical spectrum analyser by incrementally raising the pump power up to 159.40 mW, as depicted in Figure 12. The Q-switched spectrum exhibits a central wavelength of 1565.0 nm, accompanied by a peak power of -19.996 dBm. The occurrence of an unstable Q-switched fibre laser was observed upon further increasing the pump power beyond the threshold of 159.40 mW. The investigation focused on analysing the performance of the Q-switched system under a fixed wavelength while varying the pump power [11].

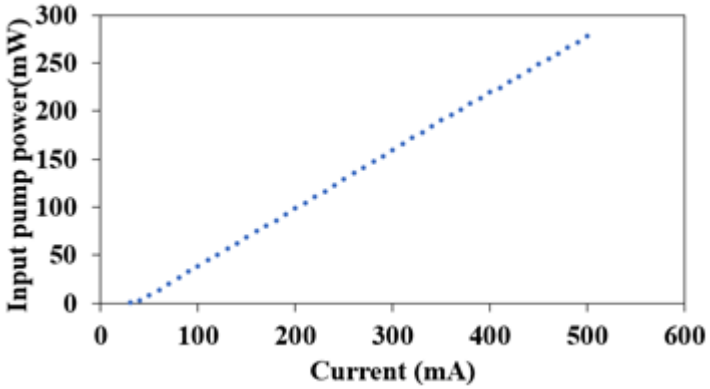


**Fig. 10** *The relationship between current and input pump power at 980nm laser diode*

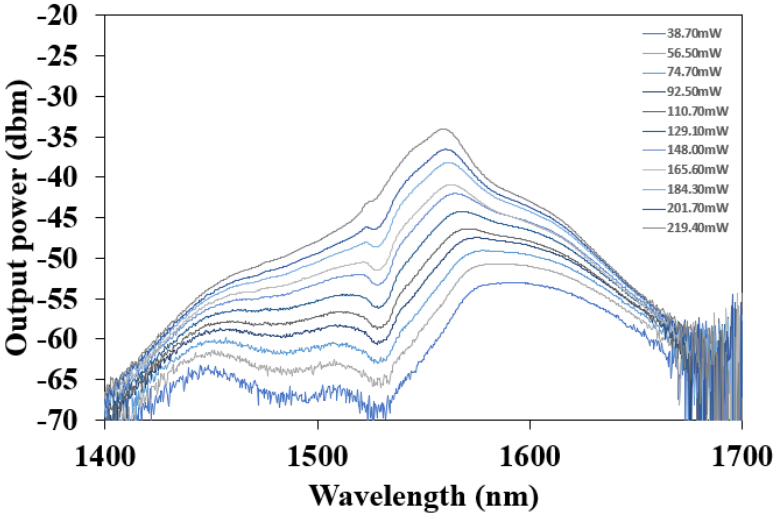


**Fig. 11** *Laser emission spectrum of EDF at 1558.4nm*

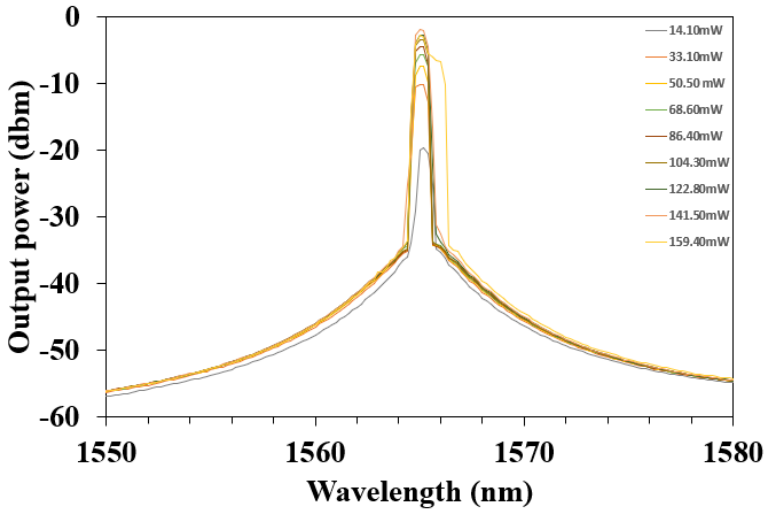


**Fig. 12** *Characterize single ring fiber laser*

## 3.3 Performance of Q-switched fiber laser using spider silk

Fig. 13(a) illustrates the spectrum of the lasing wavelength with a Q-switched configuration, represented by the blue solid line. The wavelength at the centre is approximately 1569.2 nm, with a -7.488 dB.

Fig. 13(b) displays the OSA spectra of the lasing wavelength when utilising SA, as represented by the blue solid line. The central wavelength is estimated to be around 1569.4 nm, accompanied by a -2.243 dB. A laser with a maximum pump power of 184.30 mW was utilised to achieve a stable spectrum. Once the power of the pump exceeds 184.30mW, the resulting laser spectrum becomes unstable.

Fig. 14(a) illustrates the pulse train observed at the minimum pump power of 50.50mW. The pulse train is produced with a high repetition rate of 23.3 kHz and demonstrates a brief pulse duration of 9.173μs. The temporal duration separating the two pulses is 42.33 μs. The peaks exhibit a relatively stable amplitude of approximately 0.013 V, suggesting a consistent pattern of pulse train. Nevertheless, the pulse train does not demonstrate significant amplitude fluctuations; rather, it seems to sustain a consistent form and intensity of pulses [12].

Fig. 14(b) illustrates the pulse train observed at the highest pump power level of 184.30mW. The pulse train is produced at a high frequency of 63.3 kHz and has a narrow pulse duration of 3.889 μs. The temporal duration separating the two pulses amounts to 15.98 μs. The peaks exhibit a relatively consistent amplitude of approximately 0.015 V, suggesting a stable and uniform pulse train [12].

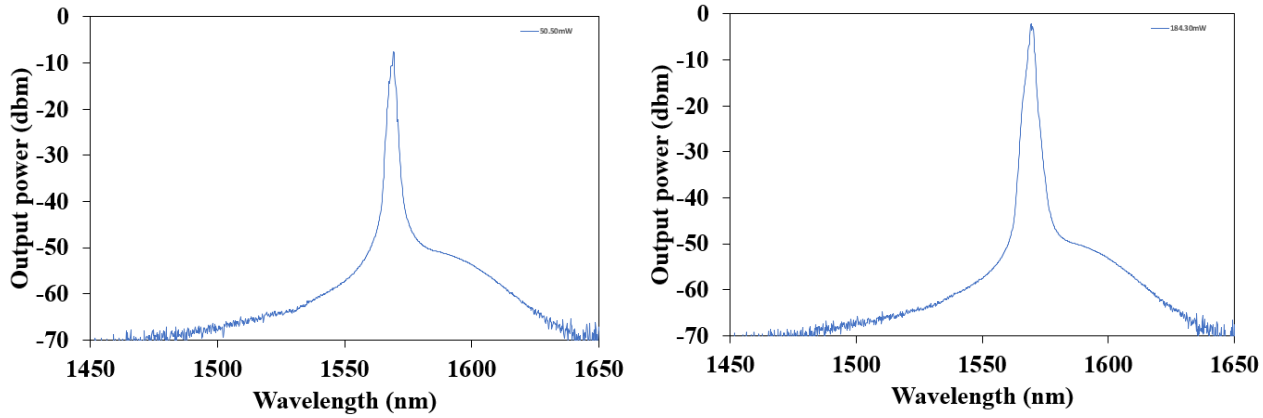


**Fig. 13** *(a) Spectrum Q-switched with minimum pump power (50.50mW) (b) Spectrum Q-switched with maximum pump power (184.30mW)*

Enhanced Knowledge in Sciences and Technology Vol. 4 No. 2 (2024) p. 417-427

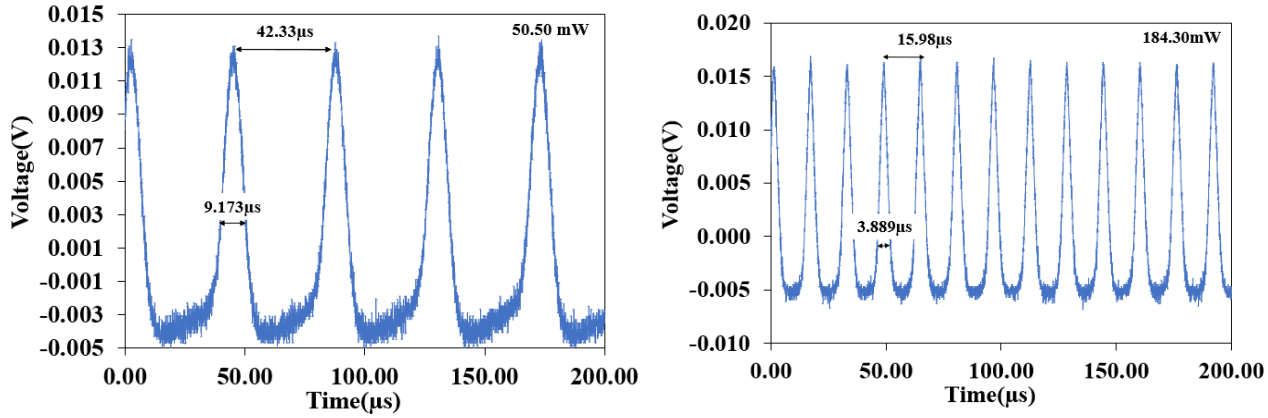


**Fig. 14** *(a) Typical pulse train at minimum pump power of 50.50mW (b) Typical pulse train at maximum pump power of 184.30mW*

Based on the data depicted in Fig. 15(a), the fundamental frequency is determined to be 23.3 kHz. Furthermore, the signal-to-noise ratio (SNR) has been calculated to be 56.21 dB, with a frequency span of 200 kHz and a resolution bandwidth of 200 Hz. The measurement was acquired using a pump power of 50.50 mW. Moreover, the examination of the radio frequency (RF) pertaining to the laser cavity has failed to detect any frequency constituent apart from the multiples of the primary frequency.

Fig. 15(b) shows the maximum frequency is measured to be 63.3 kHz. In addition, the calculation of the signal-to-noise ratio (SNR) yielded a value of 51.25 dB, given a frequency span of 200 kHz and a resolution bandwidth of 200 Hz. The measurement was obtained with a pump power of 184.30 mW.

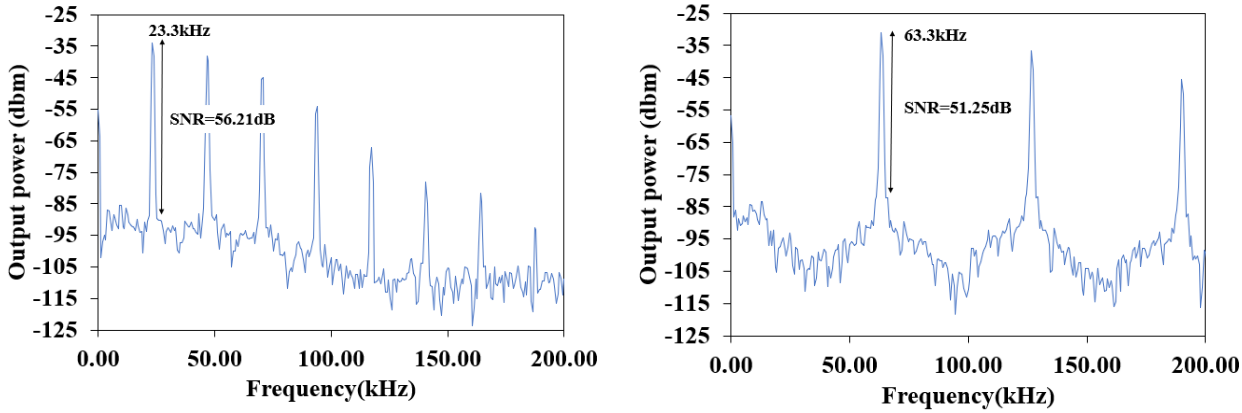


**Fig. 15** *(a)RF spectrum at the minimum pump power of 50.50mW. (b) RF spectrum at the maximum pump power of 184.30mW.*

The investigation focuses on the examination of both the repetition rate and pulse width of a Q-switched pulse fiber laser. The pump power used in this study ranges from 50.50 mW to 184.30 mW. In Fig. 16(a), it can be observed that the repetition rate has been raised from 23.3 to 63.3 kHz, while the pulse width has been reduced from 9.173 to 3.889 µs. This change in repetition rate and pulse width corresponds to an increase in pump power from 50.50 to 184.30 mW. The findings of this study indicate that the minimum pulse width of 3.889 µs exhibits a slight increase in duration, suggesting that there is potential for improvement through the reduction of the cavity length [12].

Fig. 16(b) depicts the patterns observed in the average output power and pulse energy, which exhibit a resemblance to the repetition rate. The average output power exhibited an upward trend as the pump power increased, while the pulse energy demonstrated a corresponding decrease, aligning with anticipated outcomes. The mean output power demonstrates an increase from 0.048 to 0.074 mW, leading to a corresponding alteration in pulse energy from 2.05 to 1.162 nJ.

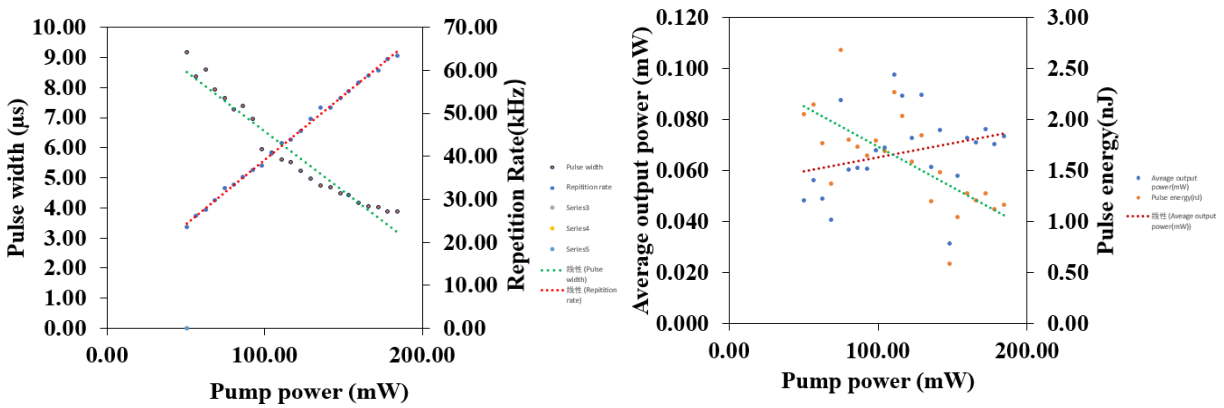


**Fig. 16** *(a)The relationship between repetition rate and pulse width against pump power (b)The relationship between average output power and pulse energy against pump power*

## 4. Conclusion

The characterization shows result Q-switched started from current pump power which is 120mA and stable until 340mA. The wavelength at the centre is almost 1569.2 nm for minimum pump power and maximum pump power. The pulse train observed at the minimum pump power of 50.50mW is produced with a high repetition rate of 23.3 kHz and a brief pulse duration of 9.173μs. The highest repetition rate is 63.3kHz and the pulse width is 3.889 μs is produced with the highest pump power level of 184.30mW. This means that there is potential for improvement through the reduction of cavity length. Furthermore, the signal-to-noise ratio (SNR) has been calculated to be 56.21 dB at a pump power of 50.50 mW while the signal-to-noise ratio (SNR) yielded a value of 51.25 dB was obtained with a pump power of 184.30 mW. The repetition rate has been raised from 23.3 to 63.3 kHz, while the pulse width has been reduced from 9.173 to 3.889 μs. This change in repetition rate and pulse width corresponds to an increase in pump power from 50.50 to 184.30 mW. The mean output power demonstrates an increase from 0.048 to 0.074 mW, leading to a corresponding alteration in pulse energy from 2.05 to 1.162 nJ. As a result, the performance of spider silk shows that the graph is stable and the result obtain is suitable to use as fiber laser.

## Acknowledgement

The authors would like to thank the Faculty of Applied Sciences and Technology, Universiti Tun Hussein Onn Malaysia, for its support in completing this project.

## Conflict of Interest

Authors declare that there is no conflict of interests regarding the publication of the paper.

## Author Contribution

*The authors confirm contribution to the paper as follows:* ***study conception and design, data collection, methodology, analysis and interpretation of results:*** *Ong Kah Yong and Noor Ummi Hazirah Hani Zalkepali. All authors reviewed the results and approved the final version of the manuscript.*

## References

[1] Radzi, N. M., Latif, A. A., Ismail, M. F., Liew, J. Y. C., Wang, E., Lee, H. K. & Ahmad, H. (2020). Q-switched fiber laser based on CdS quantum dots as a saturable absorber. Results in Physics, 16, 103123.
[2] Al-Hayali, S. K. M., Mohammed, D. Z., Khaleel, W. A. & Al-Janabi, A. H. (2017). Aluminum oxide nanoparticles as saturable absorber for C-band passively Q-switched fiber laser. Applied optics, 56(16), 4720-4726.
[3] Al-Alimi, A. W., Yusoff, N. M., Cholan, N. A., Alresheedi, M. T., Abas, A. F., Talib, Z. A. & Mahdi, M. A. (2022). Q-switched fiber laser employing a passive polarization-maintaining thulium-doped fiber as a saturable absorber. Results in Physics, 33, 105167.
[4] Chen, H., Chen, Y., Yin, J., Zhang, X., Guo, T. & Yan, P. (2016). High-damage-resistant tungsten disulfide saturable absorber mirror for passively Q-switched fiber laser. Optics express, 24(15), 16287-16296.
[5] Mao, D., Cui, X., Zhang, W., Li, M., Feng, T., Du, B. & Zhao, J. (2017). Q-switched fiber laser based on saturable absorption of ferroferric-oxide nanoparticles. Photonics Research, 5(1), 52-56.
[6] Al-Dabagh, Z. A. I. (2018). Antimony Telluride as a Saturable Absorber for Generating Q-Switched and Mode-Locked Erbium-Doped Fiber Lasers (Doctoral dissertation, University of Malaya (Malaysia)).

[7] Du, J., Wang, Q., Jiang, G., Xu, C., Zhao, C., Xiang, Y. & Zhang, H. (2014). Ytterbium-doped fiber laser passively mode locked by few-layer Molybdenum Disulfide (MoS2) saturable absorber functioned with evanescent field interaction. Scientific reports, 4(1), 6346.
[8] Niu, K., Chen, Q., Sun, R., Man, B. & Zhang, H. (2017). Passively Q-switched erbium-doped fiber laser based on SnS 2 saturable absorber. Optical Materials Express, 7(11), 3934-3943.
[9] Tian, X., Luo, H., Wei, R., Liu, M., Yang, Z., Luo, Z. & Qiu, J. (2019). Ultrafast and broadband optical nonlinearity in aluminum doped zinc oxide colloidal nanocrystals. Nanoscale, 11(29), 13988-13995.
[10] Zalkepali, N. U. H. H., Awang, N. A., Latif, A. A., Zakaria, Z., Yuzaile, Y. R. & Mahmud, N. N. H. E. N. (2020). Switchable dual-wavelength Q-switched fiber laser based on sputtered indium tin oxide as saturable absorber. Results in Physics, 17, 103187.
[11] Zalkepali, N. U. H. H., Awang, N. A., Yuzaile, Y. R., Zakaria, Z., Latif, A. A., Ali, A. H. & Mahmud, N. N. H. E. N. (2019). Indium tin oxide thin film based saturable absorber for Q-switching in C-band region. In Journal of Physics: Conference Series (Vol. 1371, No. 1, p. 012018). IOP Publishing.
[12] Muhammad, N. A. M., Awang, N. A., Basri, H., Abd Latif, A., Zalkepali, N. U. H. H., Zamri, A. Z. M. & Mahmud, N. N. H. E. N. (2024). Steady Q-switched erbium-doped fiber laser pulse generation by exploiting spider silk as a passive saturable absorber. Optics & Laser Technology, 169, 110170.